PSEUDO NEGATIVE STIFFNESS CONTROL OF THE BENCHMARK CABLE-STAYED BRIDGE

Hirokazu IEMURA[1] and Mulyo Harris Pradono[2]

Abstract

Effectiveness of variable damper employing pseudo negative stiffness control on the benchmark cable-stayed bridges was studied. Combination of pseudo negative stiffness hysteretic loop produced by variable damper plus elastic stiffness of the deck-tower connections produces hysteretic loop that approaches rigid perfectly-plastic force-deformation characteristics which has large damping ratio. The advantage is that sensors are required only at damper connections to measure relative displacements. Comparisons are made between passive, pseudo negative stiffness, and active control for the benchmark bridge. The results of pseudo negative stiffness control are significantly better than those of passive control and comparable to those of active control.

Introduction

Cable-stayed bridges are very appealing aesthetically and also very important lifeline structures. The increasing popularity of these bridges can be attributed to the appealing aesthetics, full and efficient utilization of structural materials, increased stiffness over suspension bridges, efficient and fast mode of construction, and relatively small size of substructure (Nazmy and Abdel-Ghaffar, 1987). However, from the structural dynamics point of view, cable-stayed bridges exhibit complex behavior in which the vertical, translational, and torsional motions are often strongly coupled (Caicedo et al., 2002). These flexible structures raise many concerns about their behavior under environmental dynamic loads such as wind, earthquake, and vehicular traffic-loads. From the analyses of various observational data, it is known that these bridges have very small mechanical or structural damping (0.3% - 2%) (Abdel-Ghaffar, 1991).

The fact that cable-stayed bridges possess little damping characteristics to help alleviate vibration under severe ground motions, wind turbulence, and traffic loadings spurred recent efforts to enhance the technology of structural control, whether it is active, passive, semi-active or combination thereof to alleviate dynamic responses. One of the significant demerits of active control is the large amount of energy required to reduce vibration of large structural systems. Moreover, many active control systems for civil engineering applications operate primarily to modify structural damping, preliminary studies indicate that semi-active control strategies can potentially achieve the majority of the performance of fully active systems (Spencer et al., 1997). Therefore, semi-active

[1] Professor, Dept. of Urban Management, Kyoto University, Kyoto
[2] Post-doctoral Fellow, Dept. of Urban Management, Kyoto University, Kyoto

control technologies have recently been widely investigated to reduce the dynamic response of structures subjected to earthquake and wind excitations (Spencer et al., 1997; Housner et al., 1997; Patten, 1998; Kurata et al., 1999; Jung et al., 2001; He et al., 2001).

Semi-active control in seismically excited structures is mainly to dissipate energy from the structure. Therefore, semi-active control with much simpler algorithm will be used to increase the energy dissipated by variable dampers. The authors use pseudo negative stiffness control algorithm (Iemura et al., 2001; Iemura et al., 2003; Iemura and Pradono, 2003; Iemura and Pradono, 2002) to improve the hysteretic loop produced by variable dampers. The application of this control method to the Phase II benchmark control problem of cable-stayed bridges is investigated and the results are compared to those by passive and active control.

Pseudo Negative Stiffness Hysteretic Loops

It has been reported in (Iemura et al., 2001; Iemura et al., 2003; Iemura and Pradono, 2003; Iemura and Pradono, 2002) that pseudo-negative stiffness hysteretic loop is effective in reducing seismic responses. The pseudo negative stiffness hysteretic loop was produced by variable orifice oil damper. By using this device, opening ratio of the flow control can be changed by electric power based on signal from control PC and the quantity of flow through valve can be adjusted. This series of mechanism enables variable damper to generate the demanded force as close as possible. From an experimental result of a typical variable orifice oil damper, relationship among damping force, opening ratio, and relative velocity can be written as follows:

$$F(h,\dot{u}_{dev}) = \mathrm{sgn}(\dot{u}_{dev})\left\{\left(\frac{159.232}{h^2}+307.2\right)\dot{u}_{dev}^2+0.6\right\}\ (\mathrm{kN}) \qquad (1)$$

where F is the damping force that is a function of piston velocity $\dot{u}_{dev}$ and valve opening ratio h. In other words, damping force is a function of both opening ratio and piston velocity. The feasible region of the variable damper is shown in Figure 1. Damping force of variable damper is in the same direction of relative velocity, therefore, second and forth quadrants in the figure are impossible region of damping force.

Value of opening ratio is decided at every time step on the condition as follows. (i) Case of the demanded force in the feasible region II; Opening ratio h is calculated based on Equation (1) from the demanded force and measured relative velocity. The signal of opening ratio is set for variable damper to generate the demanded force. (ii) Case of the demanded force outside the feasible region II; When the direction of the demanded force is the same to that of relative velocity, opening ratio is chosen for variable damper to generate demanded force. When the direction of the demanded force is against that of relative velocity, opening ratio is chosen to generate as small force as possible. Experimental result of pseudo negative stiffness hysteretic loop produced by variable orifice oil damper is shown in Figure 2.

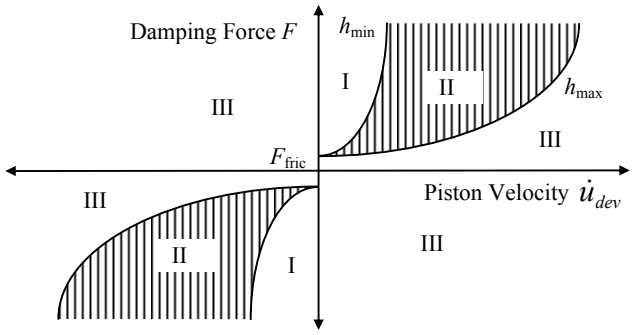

Figure1. Feasible region of variable damper in piston velocity and damping force plane

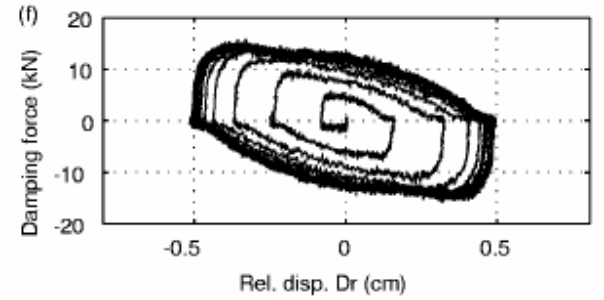

Figure 2. Experimental results of variable orifice oil damper controlled with pseudo negative stiffness algorithm subjected to sinusoidal input (Iemura et al., 2001)

The pseudo negative stiffness algorithm has great advantage in practical application. Only relative displacement and velocity are used for feedback and sensor is required only at damper place. A simple algorithm (shown afterwards) and relatively few sensors reduce the source of errors and uncertainties.

The demanded force is calculated by using simple algorithm shown in Equation (2). Because of the limitations of damping devices (they can only produce force opposite to the direction of movement), then Equation (3) applies. The demanded force is graphically shown in Figure 4a.

$$f_c = k_{neg} u_{dev} + c_s \dot{u}_{dev} \tag{2}$$

$$f_{Dc} = \begin{cases} \text{smallest possible force} & f_c \dot{u}_{dev} < 0 \\ f_c & f_c \dot{u}_{dev} > 0 \end{cases} \tag{3}$$

where f_c is the negative stiffness force with damping, and f_{Dc} is the demanded force that can be realized by variable damper. c_s and k_{neg} are selected damping coefficient and selected negative stiffness, respectively. u_{dev} and $\dot{u}_{dev}$ are displacement and velocity across the damper, respectively.

The advantage of pseudo negative stiffness hysteretic loop in reducing structural dynamic response will be illustrated. Consider a steady-state motion of an SDOF system. The graphical interpretation for the energy dissipated in viscous damping is shown as a hysteretic loop in Figure 3a (Chopra, 1995). It is of interest to examine the total (elastic plus damping) resisting force because additional dampers are usually put parallel to existing members that are assumed to be elastic. The plot is the hysteretic loop of Figure 3a rotated as shown in Figure 3b. Where f_D and f_S are damping and elastic forces, respectively, u and $\dot{u}$ are relative displacement and velocity, respectively, ω is excitation frequency and u_0 is maximum relative displacement. The energy dissipated by damping is still the area enclosed by the ellipse. The hysteretic loop associated with viscous damping is the result of dynamic hysteretic, therefore the loop area is proportional to excitation frequency. This has advantage over static hysteretic associated with plastic deformation since no permanent displacement is expected at the end of excitation.

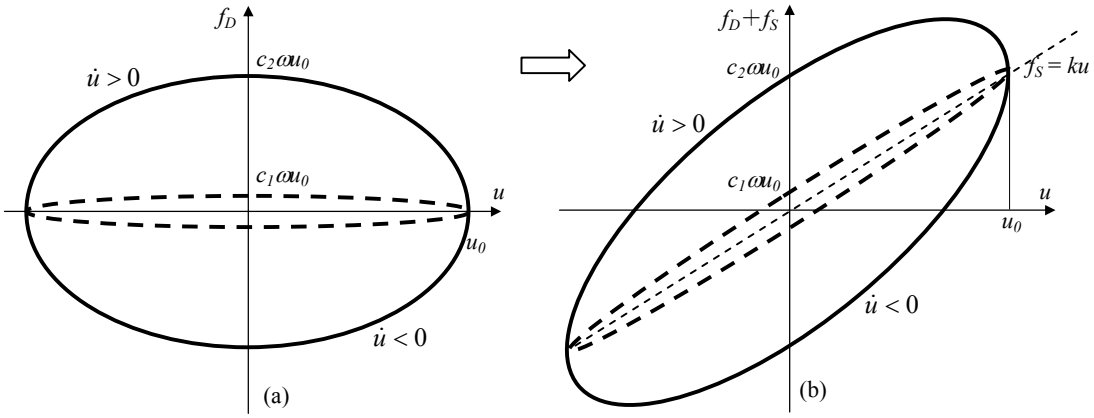

Figure 3. Hysteretic loop for (a) viscous damper; (b) spring and viscous damper is parallel

It is clear from Figure 3 that increasing the damping coefficient from c_1 to c_2 will increase the energy dissipation. However, as damping coefficient increases, the maximum total (elastic plus damping) resisting force become larger than the maximum elastic force (Figure 3b). For a harmonic motion of an SDOF system, the elastic plus damping force can be calculated as follows. For a linear viscous damper shown in Figure 3b, damping force is expressed as (Chopra, 1995)

$$f_D = c_{cr}\zeta\omega\sqrt{u_0^2 - u^2} \tag{4}$$

where ζ is damping ratio. The frequency of the excitation ω is the same as the natural frequency of the system. The critical damping coefficient c_{cr} can then be expressed as

$$c_{cr} = \frac{2k}{\omega} \tag{5}$$

where k is the existing elastic stiffness. Therefore, Equation (4) can be rewritten as

$$f_D = 2\zeta k\sqrt{u_0^2 - u^2} \tag{6}$$

The total of elastic force plus damping force is expressed as

$$f = ku + 2\zeta k\sqrt{u_0^2 - u^2} \tag{7}$$

Maximum total force occurs when,

$$\frac{df}{du} = k - \frac{2\zeta ku}{\sqrt{u_0^2 - u^2}} = 0 \tag{8}$$

or,
$$u_{f,\max} = \frac{u_0}{\sqrt{4\zeta^2 + 1}} \tag{9}$$

where $u_{f,\max}$ is the displacement at the maximum total force. Therefore, the ratio of maximum total force $f_{\max}$ divided by maximum elastic force $f_{s,\max}$ can then be expressed as

$$\frac{f_{\max}}{f_{s,\max}} = \frac{\frac{ku_0}{\sqrt{4\zeta^2+1}} + 2\zeta ku_0\sqrt{1 - \frac{1}{4\zeta^2+1}}}{ku_0} = \sqrt{4\zeta^2 + 1} \tag{10}$$

By using Equation (10), the ratio between maximum damping plus elastic force and maximum elastic force can be calculated. For example, for a damping ratio ζ of 0.5, then the total (damping + elastic) force will be 1.414 times the elastic force.

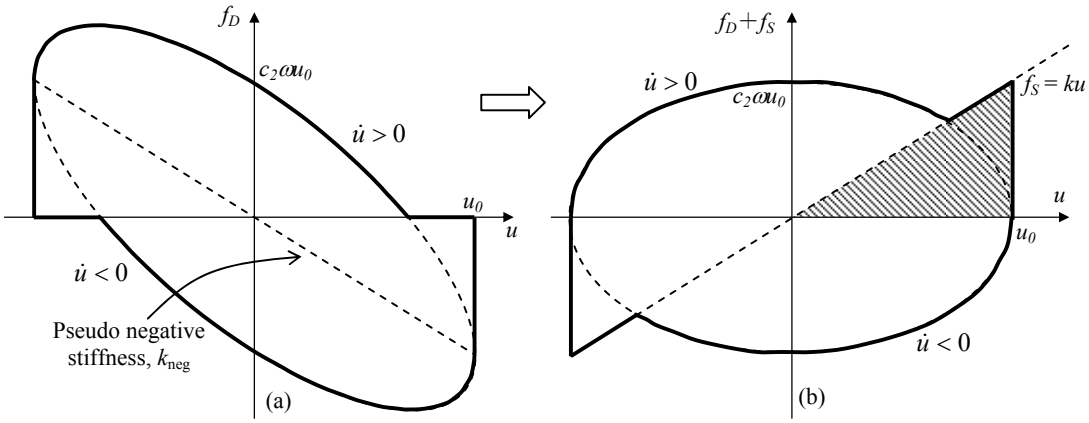

Figure 4. Hysteretic loop for (a) variable damper; (b) spring and variable damper is parallel

Looking at the above fact, it is intended herein to increase the energy dissipated without increasing the maximum total restoring force by using the pseudo negative stiffness hysteretic loop as illustrated in Figure 4. It is again of interest to examine the total (elastic plus damping) resisting force. The plot is the hysteretic loop of Figure 4a rotated

as shown in Figure 4b. It is clear from the figure that large energy can be dissipated while keeping the maximum total resisting force significantly lower than those in linear viscous damper case (Figure 3).

The maximum strain energy E_{so} of the SDOF system is shown graphically as shaded area in Figure 4b, and the energy loss in a cycle of harmonic vibration E_D is an area inside the thick loop. The equivalent damping ratio ζ_{eq} is from Equation (11) (Chopra, 1995).

$$\zeta_{eq} = \frac{1}{4\pi}\frac{E_D}{E_{so}} \tag{11}$$

For the hysteretic loop shown in Figure 4b, Equation (11) can be rewritten as

$$\zeta_{eq} = \frac{\pi c\omega u_0^2 + c\omega u_0^2 - 0.25\pi c\omega u_0^2}{2\pi k u_0^2} \tag{12}$$

$$\zeta_{eq} = \frac{c\omega u_0^2 (0.75\pi + 1)}{2\pi c\omega u_0^2} \tag{13}$$

$$\zeta_{eq} = \frac{0.75\pi + 1}{2\pi} = 0.534 \tag{14}$$

The calculation is shown in Equations (12) to (14) and end up with 53.4% damping ratio which is close to 64% damping ratio of rigid-perfectly plastic force-deformation characteristics (Priestley et al., 1996), with no residual displacement. On the other hand, for the same damping ratio as 53.4%, hysteretic loop in Figure 3b (linear viscous damper) will produce total force of 1.46 times the elastic force (calculated with Equation (10)).

Benchmark Problem Statement

The second phase of benchmark structural control problem for cable-stayed bridges have been introduced in (Caicedo et al., 2002). The problems are available for downloading on the benchmark web site in *http://wusceel.cive.wustl.edu/quake/*. The cable-stayed bridge used for this benchmark study is the Bill Emerson Memorial Bridge spanning the Mississippi River (on Missouri 74 – Illinois 146) near Cape Girardeau, Missouri.

The first ten frequencies (shown also as natural period in bracket) of the evaluation model are 0.2899 (3.45 s), 0.3699 (2.70 s), 0.4683 (2.14 s), 0.5158 (1.94 s), 0.5812 (1.72 s), 0.6490 (1.54 s), 0.6687 (1.50 s), 0.6970 (1.44 s), 0.7102 (1.41 s), and 0.7203 Hz (1.39 s). To make it possible to place devices acting longitudinally between the deck and the tower, a modified evaluation model is formed in which the connections between the tower and the deck are disconnected. The control devices should connect the deck to the tower.

The frequencies of this second model are much lower than those of the nominal bridge model. The first ten frequencies of this second model are 0.1618 (6.18 s), 0.2666 (3.75 s), 0.3723 (2.69 s), 0.4545 (2.20 s), 0.5015 (1.99 s), 0.5650 (1.77 s), 0.6187 (1.61 s), 0.6486 (1.54 s), 0.6965 (1.43 s), and 0.7094 Hz (1.41 s).

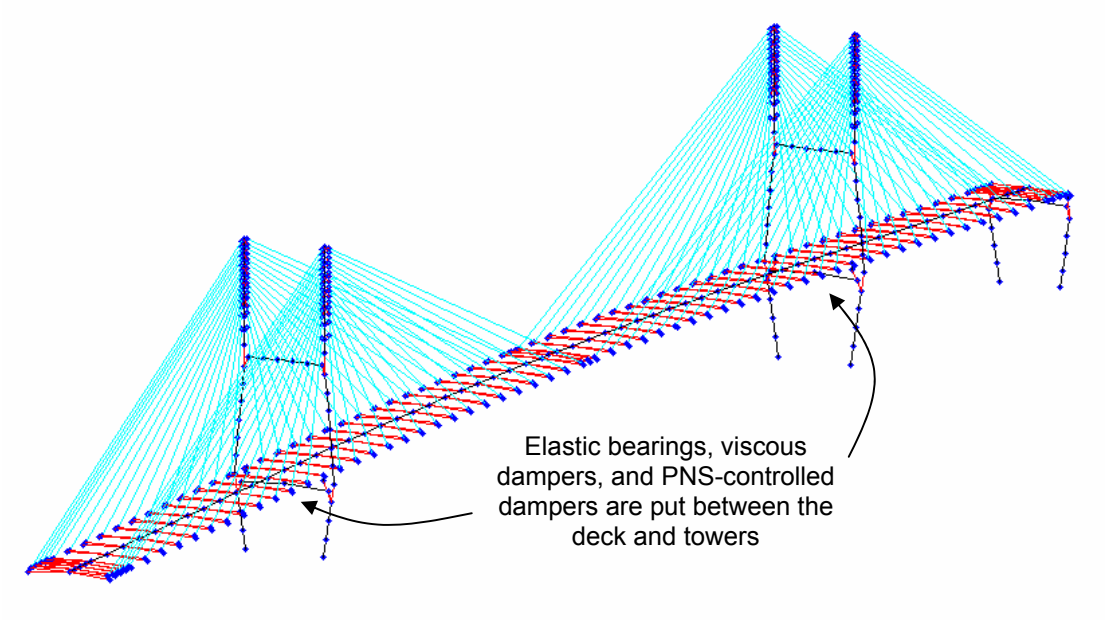

Figure 5. Bill Emerson Memorial Bridge Evaluation Model

A set of 18 criteria have been developed to evaluate the capabilities of each control strategy (Caicedo et al., 2002). The first six evaluation criteria consider the ability of the controller to reduce peak responses, the second five criteria considered normed responses over the entire time record, and the last seven criteria consider the requirements of the control system itself.

Passive Control System

The passive control system employs a total of 16 viscous dampers located between the deck and the towers (eight between the deck and pier 2, and eight between the deck and pier 3; piers 2 and 3 are regarded as towers) and oriented to apply forces longitudinally. For simplicity, the damper force is linearly proportional to the piston velocity. It is important to check the appropriate damping coefficient related to this passive systems of the bridge. This can be done by altering the damping coefficient. The results are shown in Figure 6 for total damping coefficient from 0 to 4000 kN/m/s for four dampers.

It is clear from the figure that increasing damping coefficient of the viscous damper will decrease the deck displacement, although the relation is not linear. On the other hand,

increasing damping coefficient may increase the seismic induced force (for example tower base shear for Gebze input earthquake). Therefore, a damping coefficient of 2000 kN/m/s per four dampers is assumed to be appropriate. The evaluation criteria based on these additional viscous dampers is shown in Table 1.

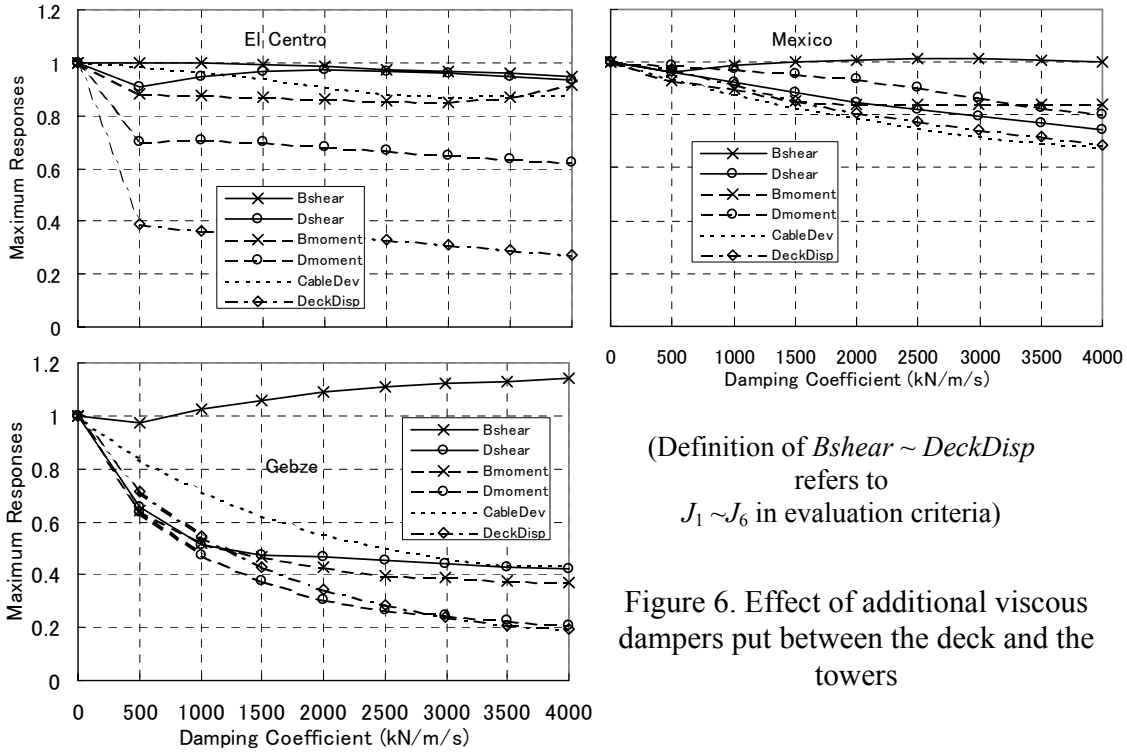

(Definition of *Bshear* ~ *DeckDisp* refers to J_1 ~J_6 in evaluation criteria)

Figure 6. Effect of additional viscous dampers put between the deck and the towers

Table 1. Evaluation criteria based on linear viscous dampers put between the deck and the towers

Evaluation Criteria	El Centro	Mexico	Gebze
J_{1x} (shear force at tower base(X))	0.323	0.365	0.385
J_{1z} (shear force at tower base(Z))	1.014	1.108	1.035
J_{2x} (shear force at deck level(X))	0.920	0.989	1.085
J_{2z} (shear force at deck level(Z))	0.962	0.999	0.995
J_{3x} (moment at tower base(X))	0.235	0.314	0.441
J_{3z} (moment at tower base(Z))	1.096	1.070	1.040
J_{4x} (moment at deck level(X))	0.549	0.810	1.300
J_{4z} (moment at deck level(Z))	1.009	0.993	0.999
J_5 (deviation of cable tension)	0.247	0.131	0.225
J_6 (deck displacement)	1.075	1.710	4.865
J_{7x} (normed shear force at tower base(X))	0.226	0.254	0.272
J_{7z} (normed shear force at tower base(Z))	1.002	1.048	1.042
J_{8x} (normed shear force at deck level(X))	0.899	0.933	1.145
J_{8z} (normed shear force at deck level(Z))	0.978	0.997	0.990
J_{9x} (normed moment at tower base(X))	0.231	0.275	0.463

J_{9z} (normed moment at tower base(Z))	0.997	1.045	1.031
J_{10x} (normed moment at deck level(X))	0.703	0.870	1.473
J_{10z} (normed moment at deck level(Z))	1.002	1.004	1.002
J_{11} (normed deviation of cable tension)	0.027	0.017	0.022
J_{12x} (force by control devices(X))	1.597e-3	0.983e-3	2.077e-3
J_{12z} (force by control devices(Z))	0.000e+0	0.000e+0	0.000e+0
J_{13x} (stroke of control devices(X))	0.531	0.754	2.072
J_{13z} (stroke of control devices(Z))	0.000	0.000	0.000
J_{16} (number of control devices)	16	16	16
J_{17} (number of sensors)	0	0	0

From the table, Gebze earthquake results in large displacement response. This matter is in the authors' expectation, as a study by the authors (Iemura and Pradono, 2002) shows that additional stiffness is needed between the deck and the towers so that excessive displacement can be minimized, but of course in the expense of increasing member forces.

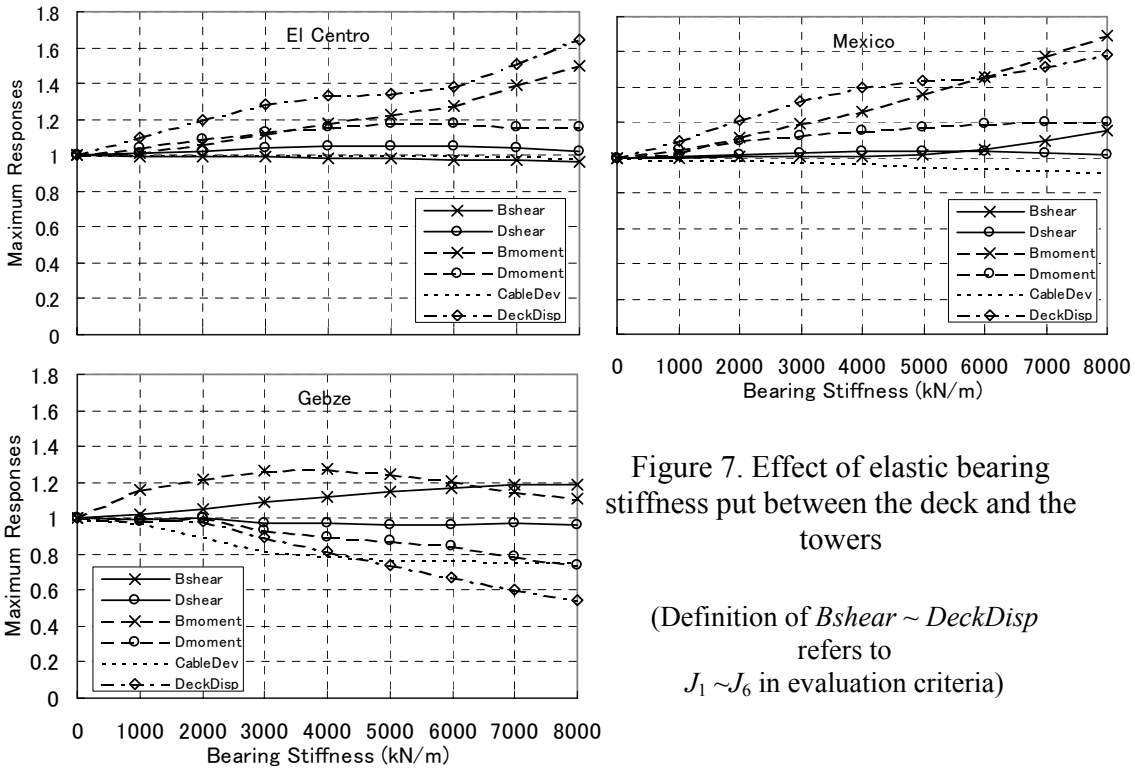

Figure 7. Effect of elastic bearing stiffness put between the deck and the towers

(Definition of *Bshear* ~ *DeckDisp* refers to J_1 ~J_6 in evaluation criteria)

To reduce the excessive displacement, elastic bearings are added parallel to the above viscous dampers in the longitudinal direction. It will be checked how much stiffness is needed between the deck and the towers. The stiffness of one bearing is varied from 1000 kN/m to 8000 kN/m. The results are shown in Figure 7. From the figure, it was decided to use four bearings with stiffness of 8000 kN/m each, because the displacement response of Gebze earthquake can be reduced significantly, with the expense of some increment in member forces. The evaluation criteria based on additional damping and stiffness is shown

in Table 2 (at 'passive' columns).

Pseudo Negative Stiffness Control System

The pseudo negative stiffness (PNS) control system employs a total of 16 variable dampers located between the deck and the towers (eight between the deck and pier 2, and eight between the deck and pier 3, piers 2 and 3 are regarded as towers) and oriented to apply forces longitudinally. The assumption is that elastic bearings used for the passive system is also applied herein. Displacement transducers are used for feedback to the control algorithm. Two displacement sensors are positioned between the deck and pier 2, and two between the deck and pier 3, which make a total of four displacement sensors. All displacement measurements are obtained in the longitudinal direction to the bridge. For simplicity, the control devices act as ideal dampers, and damper dynamics and control-structure interaction is neglected.

The force command for the variable damper is expressed in Equations (2) and (3). The negative stiffness value (k_{neg}) in Equation (2) to control the variable damper is chosen as –8000 kN/m, because k_{neg} that equals negative of the existing stiffness (in this case bearing stiffness) gives the smallest damping plus elastic force (see Figure 4). The damping coefficient c_s is set to be the same with the passive viscous damping case, that is 2000 kN/m/s.

The evaluation criteria based on the pseudo negative stiffness control system are shown in Table 2 (at 'pns' columns). It is clear from the table that pseudo negative stiffness control reduces seismic responses better than those by passive control.

Table 2. Evaluation criteria based on passive and pseudo negative stiffness control methods

Evaluation Criteria	ElCentro		Mexico		Gebze	
	passive*	pns**	passive*	pns**	passive*	pns**
J_{1x} (shear at tower base(X))	**0.311**	0.324	0.423	**0.367**	0.458	**0.425**
J_{1z} (shear at tower base(Z))	1.023	1.016	1.107	1.106	1.033	1.033
J_{2x} (shear at deck level(X))	0.943	**0.922**	1.008	**0.967**	1.047	**0.948**
J_{2z} (shear at deck level(Z))	0.964	0.965	0.995	0.994	0.991	0.995
J_{3x} (moment at tower base(X))	0.353	**0.261**	0.530	**0.411**	**0.488**	0.505
J_{3z} (moment at tower base(Z))	1.092	1.104	1.071	1.066	1.036	1.043
J_{4x} (moment at deck level(X))	0.635	**0.540**	0.971	**0.890**	0.959	**0.833**
J_{4z} (moment at deck level(Z))	1.009	1.007	0.993	0.992	1.000	1.000
J_5 (deviation of cable tension)	0.244	**0.218**	**0.120**	0.121	**0.171**	0.184
J_6 (deck displacement)	1.768	**1.139**	2.715	**2.038**	2.654	**2.605**
J_{7x} (nor. shear @tower base(X))	0.249	**0.232**	0.330	**0.288**	0.360	**0.314**
J_{7z} (nor. shear @tower base(Z))	1.007	0.998	1.047	1.044	1.041	1.034
J_{8x} (nor. shear @deck level(X))	0.911	**0.861**	1.076	**0.914**	1.001	**0.931**
J_{8z} (nor. shear @deck level(Z))	0.977	0.978	0.998	0.997	0.990	0.989
J_{9x} (nor. mom. @tower base(X))	0.298	**0.244**	0.474	**0.326**	0.509	**0.422**

J_{9z} (nor. mom. at tower base(Z))	1.001	0.995	1.045	1.041	1.031	1.026
J_{10x} (nor. mom. @deck level(X))	0.730	**0.666**	1.091	**0.869**	0.858	**0.767**
J_{10z} (nor. mom. @deck level(Z))	1.001	1.001	1.004	1.004	1.002	1.001
J_{11} (nor. deviation of cbl tension)	**0.024**	0.025	0.017	**0.016**	**0.015**	0.016
J_{12x} (force by devices(X))***	3.235e-3	**2.412e-3**	2.451e-3	**1.882e-3**	3.137e-3	**2.627e-3**
J_{12z} (force by devices(Z))***	0.000e+0	0.000e+0	0.000e+0	0.000e+0	0.000e+0	0.000e+0
J_{13x} (stroke of devices(X))	0.883	**0.583**	1.308	**0.942**	1.036	1.036
J_{13z} (stroke of devices(Z))	0.000	0.000	0.000	0.000	0.000	0.000
J_{16} (number of devices)****	20	20	20	20	20	20
J_{17} (number of sensors)	**0**	4	**0**	4	**0**	4

Note : * Linear viscous dampers and elastic bearings between the deck and towers
** Pseudo negative stiffness dampers and elastic bearings between the deck and towers
*** Force by four dampers plus an elastic bearing
**** 16 dampers plus four elastic bearings
Bold number shows that this type of control is better than the other one.

The reason for this better performance of pseudo negative stiffness control system is that hysteretic loop of the damper is altered from horizontal elliptical shape of linear viscous damper to become pseudo negative stiffness hysteretic loop of PNS-controlled damper. Why this is so important? Damper is usually set parallel to an existing member that has stiffness. As it has been explained in section "Pseudo Negative Stiffness Hysteretic Loop" beforehand, damper hysteretic loop that represent pseudo negative stiffness shape will produce virtually rigid perfectly-plastic force-deformation characteristics that has large damping ratio. The PNS-controlled damper hysteretic loop keeps the combined damper plus elastic force as low as possible while produces fat hysteretic loop. An illustration is drawn for this matter (Figure 8).

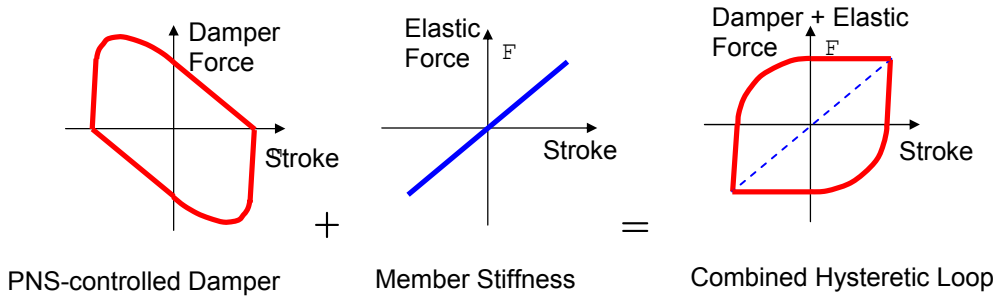

Figure 8. Combination of PNS-controlled damper plus elastic member hysteretic loops

Hysteretic loop of the passive system and pseudo negative stiffness control system is shown in Figure 9. The figure only shows hysteretic loop of the dampers. The difference of the hysteretic loops between linear viscous damper and PNS-controlled damper is clear from the figure.

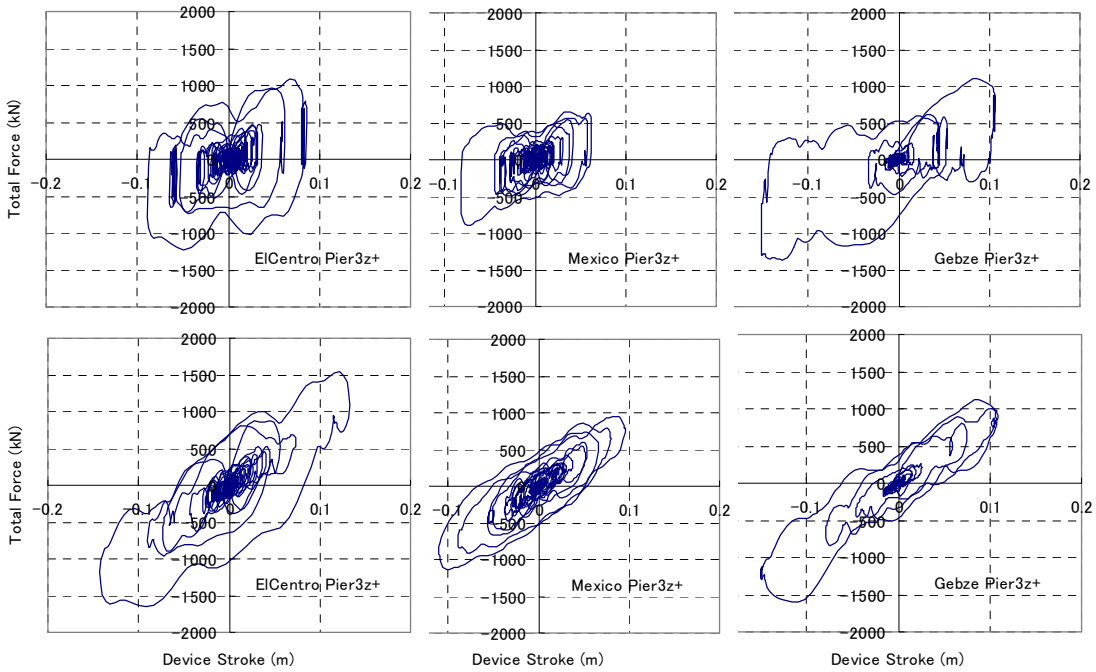

Figure 10. Combined hysteretic loops of (upper) PNS-controlled dampers plus bearings and (lower) viscous damper plus bearings

Comparison with Active Control Results

The benchmark problem contains sample active control, therefore, it is interesting to be shown herein. The control uses 24 actuators put between the deck and towers, the deck and abutment, and the deck and pier (Caicedo et al., 2002). Table 3 shows the results of active control of the benchmark control problem of cable-stayed bridges. Comparison of the results between pseudo negative stiffness control and active control shows that pseudo negative stiffness control can achieve the potential of active control. Italic numbers in the table shows that pseudo negative stiffness control has better performance than active control in reducing seismic responses, such as in shear at tower base, normed shear at deck level, force and stroke of control devices, number of devices, and number of sensors.

Table 3. Evaluation criteria based on sample active control

Evaluation Criteria	El Centro	Mexico	Gebze
J_{1x} (shear force at tower base(X))	*0.331*	*0.415*	*0.474*
J_{1z} (shear force at tower base(Z))	1.022	1.117	1.037
J_{2x} (shear force at deck level(X))	0.810	0.828	0.941
J_{2z} (shear force at deck level(Z))	0.967	0.998	0.994
J_{3x} (moment at tower base(X))	*0.324*	0.396	0.456
J_{3z} (moment at tower base(Z))	1.097	1.079	1.046
J_{4x} (moment at deck level(X))	*0.612*	0.766	*0.955*

J_{4z} (moment at deck level(Z))	1.009	0.992	1.001
J_5 (deviation of cable tension)	*0.248*	*0.121*	0.182
J_6 (deck displacement)	1.028	1.783	2.403
J_{7x} (normed shear force at tower base(X))	*0.267*	*0.327*	*0.320*
J_{7z} (normed shear force at tower base(Z))	1.014	1.056	1.053
J_{8x} (normed shear force at deck level(X))	*0.869*	*0.964*	*0.956*
J_{8z} (normed shear force at deck level(Z))	0.978	0.996	0.991
J_{9x} (normed moment at tower base(X))	*0.248*	0.319	0.400
J_{9z} (normed moment at tower base(Z))	1.006	1.053	1.039
J_{10x} (normed moment at deck level(X))	0.636	0.793	0.780
J_{10z} (normed moment at deck level(Z))	1.002	1.004	1.003
J_{11} (normed deviation of cable tension)	0.023	0.015	0.015
J_{12x} (force by control devices(X))	*2.663e-3*	1.675e-3	*2.829e-3*
J_{12z} (force by control devices(Z))	0.000e+0	0.000e+0	0.000e+0
J_{13x} (stroke of control devices(X))	*0.630*	*0.971*	*1.048*
J_{13z} (stroke of control devices(Z))	0.000	0.000	0.000
J_{16} (number of control devices)*	*24*	*24*	*24*
J_{17} (number of sensors)**	*18*	*18*	*18*

Note : *16 Actuators between the deck and towers, four between the deck and abutment, and four between the deck and pier

** 14 accelerometers and four displacement transducers

Italic number shows that PNS-controlled system produces lower number.

Conclusions

In this paper, pseudo negative stiffness (PNS) control strategy using variable dampers has been proposed by investigating the benchmark control problem for seismic responses of cable-stayed bridges. The proposed control design employs four displacement transducers, 16 variable dampers, and four isolation bearings. Simple pseudo negative stiffness algorithm is used to determine the control force for each variable damper so that combination of the damper hysteretic loop plus existing member stiffness produces rigid perfectly plastic force-deformation characteristics that has large damping ratio. Comparisons are made between passive control systems and PNS control systems. The numerical results demonstrate that the performance of the PNS control systems is significantly better than that of passive control system and is comparable to fully active system in reducing seismic responses.

Acknowledgements

Invaluable discussions with Associate Professor Dr. Akira Igarashi at Kyoto University in Japan, Dr. Akihiro Toyooka at Railway Technical Research Institute in Japan, and Professor Dr. Shirley Dyke at Washington University in Saint Louis are gratefully acknowledged.

References

Nazmy, A. S. and Abdel-Ghaffar, A. M. *Seismic Response Analysis of Cable-stayed Bridges Subjected to Uniform and Multiple-Support Excitations*, Report No. 87-SM-1, Department of Civil Engineering, Princeton University, NJ 08544, May, 1987.

Caicedo, J. M., Dyke, S. J., Moon, S. J., Bergman, L. A., Turan, G., and Hague, S. Phase II Benchmark Control Problem for Seismic Response of Cable-stayed Bridges. *http://wusceel.cive.wustl.edu/quake/*, 2002.

Abdel-Ghaffar, A. M. Cable-stayed bridges under seismic action. *Cable-stayed Bridges: Recent Developments and Their Future*, Editor: M. Ito, Elsevier Science Publishers, 1991.

Spencer, B.F., Dyke, S.J., Sain, M.K., and Carlson, J.D. Phenomenological Model for Magnetorheological Dampers. *Journal of Engineering Mechanics*, Vol. 123, No. 3, March, 1997.

Housner, G.W., Bergman, L.A., Caughey, T.K., Chassiakos, A.G., Claus, R.O., Masri, S.F., Skelton, R.E., Soong, T.T., Spencer, B.F., Yao, J.T.P. Structural Control: Past, Present, and Future. *Journal of Engineering Mechanics*, Vol. 123, No. 9, September, 1997.

Jung, H-J, Spencer, B.F., Lee, I-W. Benchmark Control Problem for Seismically Excited Cable-stayed Bridges using Smart Damping Strategies. *Proc. IABSE Conference*, Seoul, June, 2001.

He, W.L., Agrawal, A.K., and Mahmoud, K. Control of Seismically Excited Cable-stayed Bridge using Resetting Semiactive Stiffness Dampers. *Journal of Bridge Engineering*, Vol. 6, No. 6, November/December, 2001.

Patten, W.N. The I-35 Walnut Creek Bridge: An intelligent highway bridge via semi-active structural control, *Proc. 2nd World Conf. on Struct. Control*, 1, Kyoto, Japan, 1998, pp427-436.

Kurata, N., Kobori, T., Takahashi, M., Niwa, N. and Midorikawa, H. Actual seismic response controlled building with semi-active damper system, *Earthquake Engrg. and Struct. Dyn.*, 28, 1999, 1427-1447.

Iemura, H., Igarashi, A., and Nakata, N. Semi-active Control of Full-scale Structures using Variable Joint Damper System. *The Fourteenth KKNN Symposium on Civil Engineering*, Kyoto, Japan, November 5-7, 2001.

Iemura, H., Igarashi, A., and Nakata, N. Semi-active Optimal Control Test of Full-scale Structural Steel Frames with the Variable Joint Damper System, *Proc. 3rd World Conf. on Struct. Control*, Como, Italy, 2003.

Iemura, H. and Pradono, M.H. Seismic Response Control of a Cable-stayed Bridge with Passive and Semi-active Control Technologies, *Proc. 3rd World Conf. on Struct. Control*, Como, Italy, 2003.

Iemura, H. and Pradono, M. H. Passive and Semi-active Response Control of a Cable-stayed Bridge. *Journal of Structural Control*, John Wiley and Sons, Vol. 9, pp. 189-204, December, 2002.

Chopra, A. K. *Dynamics of Structures, Theory and Applications to Earthquake Engineering*, Prentice Hall, Inc., 1995.

Priestley, M. J. N., Seible, F., and Calvi, G. M. *Seismic Design and Retrofit of Bridges*. John Wiley & Sons, Inc., New York, 1996.